Available online at www.sciencedirect.com
ScienceDirect
International Journal of Thermal Sciences 48 (2009) 535–546
International Journal of Thermal Sciences
www.elsevier.com/locate/ijts

Multiple quasi-steady states in a closed loop pulsating heat pipe

Sameer Khandekar [a,*], Anant Prasad Gautam [a], Pavan K. Sharma [b]

[a] *Department of Mechanical Engineering, Indian Institute of Technology Kanpur, Kanpur 208016, India*
[b] *Reactor Safety Division, Bhabha Atomic Research Center, Mumbai 400094, India*

Received 7 November 2007; received in revised form 23 April 2008; accepted 23 April 2008

Available online 12 June 2008

Abstract

The novel fact that, keeping all the operating and boundary conditions fixed, a single loop pulsating heat pipe exhibits multiple operational quasi-steady states is reported in this paper. For a specified heat power input level and volumetric filling ratio, continuous online measurements of static pressure and temperature at crucial locations, along with flow visualization, have been carried out for more than twelve hours per experimental run of device operation. Four distinct quasi-steady states have been observed in these experimental runs. Each quasi-steady state is characterized by a unique specific two-phase flow pattern and corresponding effective device conductance, revealing the strong thermo-hydrodynamic coupling guiding the thermal performance. The quasi-steady state corresponding to best thermal performance consists of continuous unidirectional flow circulations, while the state corresponding to poor thermal performance is characterized by the intermittent bidirectional flow reversals. A temporal scaling analysis is presented to estimate the order of magnitude of the equilibrium frequency of phase change and ensuing oscillations. These order-of-magnitude estimates closely match with the experimentally observed frequencies. The spectral contents of each quasi-steady state are analyzed and it is found that dominant frequencies of flow oscillations are in the range of 0.1 to 3.0 Hz with each quasi-steady state exhibiting a characteristic power spectrum. This provides the necessary velocity scaling estimates, primary information needed for any progress in design of pulsating heat pipes.

Keywords: Pulsating heat pipes; Multiple quasi-steady states; Frequency analyses; Flow patterns; Pressure oscillations

1. Introduction

In the last decade, considerable work has been done to understand the thermo-hydrodynamic characteristics of pulsating heat pipes (PHPs) [1–4]. This device is a new addition to the family of passive two-phase heat transfer devices, e.g., heat pipes and thermosyphons. Typically, a PHP consists of a plain meandering tube of capillary dimensions with many U-turns and joined end to end (forming a closed loop) as shown in Fig. 1(a). There is no additional capillary structure inside the tube as in a conventional heat pipe. The capillary tube is first evacuated and then partially filled with a working fluid, which distributes itself naturally in the form of liquid–vapor plugs and slugs inside the tube. One end of this tube bundle receives heat, transferring it to the other end by a pulsating action of the liquid–vapor/slug-bubble system. There may exist an adiabatic zone in between. This type of heat pipe is essentially a 'non-equilibrium' heat transfer device. The performance success primarily depends on continuous maintenance or sustenance of these non-equilibrium conditions in the system. The liquid and vapor slug/bubble transport is caused by the thermally induced pressure/density pulsations inside the device and no external mechanical power is required for its operation [5–11].

To understand the fundamental thermo-hydrodynamic characteristics of PHPs, some groups have tested/analyzed one primary building block, i.e. a capillary tube two-phase fluid loop [12–14]. This has led to a better understanding of the complex thermo-hydrodynamics of a multi-turn device. The studies suggest that two-phase static and dynamic instabilities, as observed in multi-turn PHPs, are also observed in a single two-phase loop. Strong thermo-hydrodynamic coupling leads

* Corresponding author. Tel.: +91 512 2597038; fax: +91 512 2597408.
E-mail address: samkhan@iitk.ac.in (S. Khandekar).

1290-0729/$ – see front matter
doi:10.1016/j.ijthermalsci.2008.04.004

Nomenclature

A	area of cross section	m^2
D	diameter	m
h_{fg}	latent heat of vaporization	J/kg
$\bar{K}$	slip factor (v_{vap}/v_{vap})	
L	characteristic length	m
$N_{pc}\|_{eq}$	equilibrium phase change number	
P	pressure	Pa
$\dot{Q}$	heat input	W
$\dot{q}''_w$	heat flux	W/m^2
R_{th}	thermal resistance	K/W
T	temperature, also transition state	°C or K
ΔT	temperature difference	°C or K
V	volume	m^3
v	velocity	m/s
x	vapor mass fraction	

Greek symbols

α	vapor void fraction	
$\Gamma_{vap}\|_{eq}$	mass rate of vapor generation per unit volume	$kg/s\,m^3$
Ω_{eq}	equilibrium frequency of phase change	1/s
ξ_h	heated perimeter	m
ρ	density	kg/m^3
λ	thermal conductivity	W/m K

Subscripts

C	condenser
E	evaporator
liq	liquid
vap	vapor
hyd	hydraulic
2-ϕ	two-phase

Abbreviations

CW	clockwise	
CCW	counter clockwise	
CLPHP	closed loop pulsating heat pipe	
FR	filling ratio of CLPHP (V_{liq}/V_{total}) at room temperature	
ID	inside diameter	m
OD	outer diameter	m
PHP	pulsating heat pipe	
SS	steady state	

to metastable fluid conditions too. In case of a single loop, orientation with respect to the gravity vector substantially affects the thermal performance (in terms of overall thermal resistance); this effect diminishes as the number of turns increase. It can be argued that a single loop PHP operates only due to the mixture density difference in the two arms, upheader and downheader, which in-turn changes the gravitational head in the two sections. This positive driving gravitational potential head must overcome the frictional and acceleration head due to the two-phase flow for the loop to operate satisfactorily. While this argument is correct for a single loop device, a multi-turn PHP also works very satisfactorily in anti-gravity top heater mode [15,16]. In such a situation, gravity does not support the fluid movement but is, in fact, opposing it. Thus, there must be an additional driving potential available inside the system to overcome the dissipation due to friction, acceleration and gravitational pressure drops. This force is rendered by bubble pumping/collapsing action and it becomes predominant as the number of turns increase beyond a particular critical number. Mathematical modeling of these phenomena is yet to be achieved. Interestingly, a complete stop-over of fluid motion with all liquid phase collecting towards the condenser side (refer Section 3.6, Fig. 7 later), has been observed in the single loop but has never been reported in a multi-turn PHP device suggesting that the number of turns increases the level of perturbations thereby diminishing the probability of such an event to near nullity. Mathematically, for a given boundary condition, the stop-over state is one of the trivial solutions of the guiding coupled transport equation of the PHP. Also, for a given heat throughput requirement, an optimum number of turns exists for maximizing the thermal conductance. Apart from a multitude of geometrical, physical and operational variables which affect the system, the performance is also strongly linked with the flow patterns existing inside. The contribution of latent heat portion, in the overall heat transfer, depends on the exiting two-phase flow pattern in the tube [17–23].

The above studies highlight the strong non-linear nature of the device operation. Since the operation is multivariate, with complex thermo-hydrodynamic coupling, this non-linearity is the manifestation of the interplay between species transport mechanisms, i.e. mass, momentum and energy transport with the associated inherent dynamical inertia. While the idea of existence of possible multiple *quasi-steady states* in PHP operation is implicitly conjectured in some of the earlier studies through phenomenological arguments, in this communication we explicitly report their existence with convincing experimental evidence obtained on a single-loop device. (For brevity, henceforth we shall drop the term 'quasi-', when referring to 'quasi-steady states' of PHPs. It should be noted that the classical usage of the term 'steady states', which refer to truly equilibrium solutions, does not apply to the case of a PHP.)

Two-phase instabilities (static as well as dynamic instabilities), leading to possible multiple steady states, are known to occur in many industrial systems. For instance, such occurrences in single-phase loop or toroidal thermosyphons, two-phase natural circulation loops of nuclear reactors and evaporators, flow boiling in parallel channels, etc. have been reported (as reviewed in [24]). In spite of the simplicity of geometry in many of these systems, the fluid motion and dynamic properties have not been effectively formulated under different boundary conditions [25–27]. Due to strong non-linear behavior of such systems, multiple steady states appear in certain ranges of para-

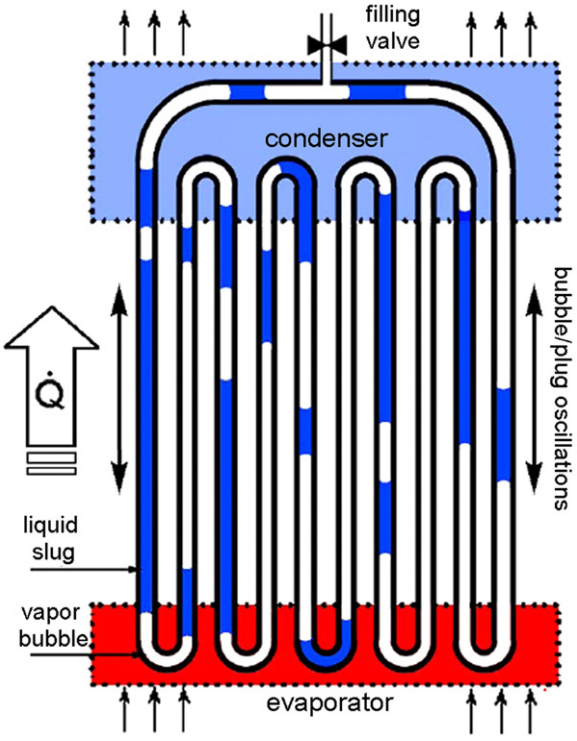

(a)

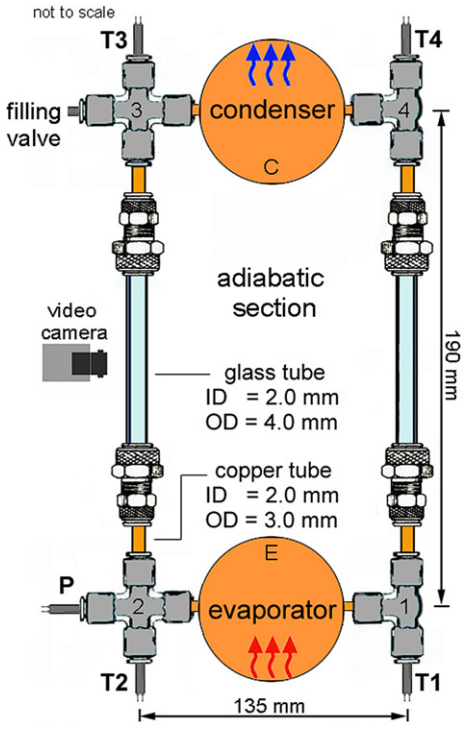

(b)

Fig. 1. (a) Schematic of a multi-turn closed loop pulsating heat pipe. (b) Schematic of the single loop pulsating heat pipe experimental setup.

metric domains. Experimental evidences have suggested that by defined setting of initial conditions and distinct perturbations to the system, some of the individual states may be externally triggered or controlled [28–30]. In addition, even a small perturbation in the operating conditions can cause the system to transit from a thermally efficient steady state to one which is thermally poor. This transition may create avalanche situation thereby drastically changing many system operating parameters such as flow pattern, wall momentum transfer coefficients, effective species transfer rates and therefore the overall desired efficiency [31,32].

In larger dimensions systems, the effect of surface tension is not pronounced; such is not the case with mini/micro two-phase systems, wherein the order of magnitude of surface tension may be predominant enough to create additional complexity [32]. Moreover, many larger systems are open in nature wherein the inlet velocity is either explicitly known or externally controlled. This is not the case in a closed loop PHP where the total mass inventory of the fluid remains constant during operation. We have tested a small scale two-phase natural circulation loop of capillary dimensions (i.e. one loop of a PHP) wherein multiple steady states have been observed. The fact that no mathematical model is still available to predict the performance of PHPs, we believe that this novel information is indeed vital for further understanding and progress.

2. Experimental setup and procedure

The experimental setup consisting of a single closed loop of capillary dimensions, partly made of copper (ID: 2.0 mm, OD: 3.0 mm) and partly of glass (ID: 2.0 mm, OD: 4.0 mm), as shown in Fig. 1(b), is designed to facilitate parametric investigations as well as simultaneous flow-visualization. The glass and copper capillary sections are connected through the four unions (1, 2, 3 and 4; make: Swagelok®) as shown in Fig. 1(b). The copper evaporator block has a 2.0 mm through hole for the fluid passage and is heated by a high heat flux surface-mountable strip heater (make: Minco®) secured by a backing plate. Condenser section, made of a hollow copper chamber, is supplied with cooling water from a constant temperature bath (make: Haake® model: DC30K20), accuracy: ±0.1 °C). Adiabatic section, between the evaporator and the condenser, is made up of the glass capillary to facilitate flow-visualization. Adequate insulation is provided on all sections. T1, T2, T3 and T4 denote four thermocouples (make: National Instruments®, Type-J, post-calibration accuracy ±0.2 °C) connected at four connecting junction unions, respectively. *P* denotes an absolute pressure transducer (make: HBM® model P3MBA, 0–5 bar, post calibration accuracy: 0.1%FS) fitted at one end of the evaporator. On the condenser side, a micro-metering valve is installed for evacuation and filling control of the working fluid. Vacuum level of less than 10^{-4} mbar is achieved inside the loop by a screw/turbine combo-pump (make: Varian®). DAQ card with signal conditioner (make: National Instruments®, NI-PCI-6024E and SC-2345) were used to facilitate simultaneous high-speed acquisition of pressure and temperature signals at 100 Hz.

For all experiments reported here, ethanol was used as the working fluid with FR $\approx 60 \pm 2\%$ which was administered using a micro-metering valve. For the current investigations, geometrical configuration was fixed with distance between evaporator and the condenser as 190 mm, and width equal to

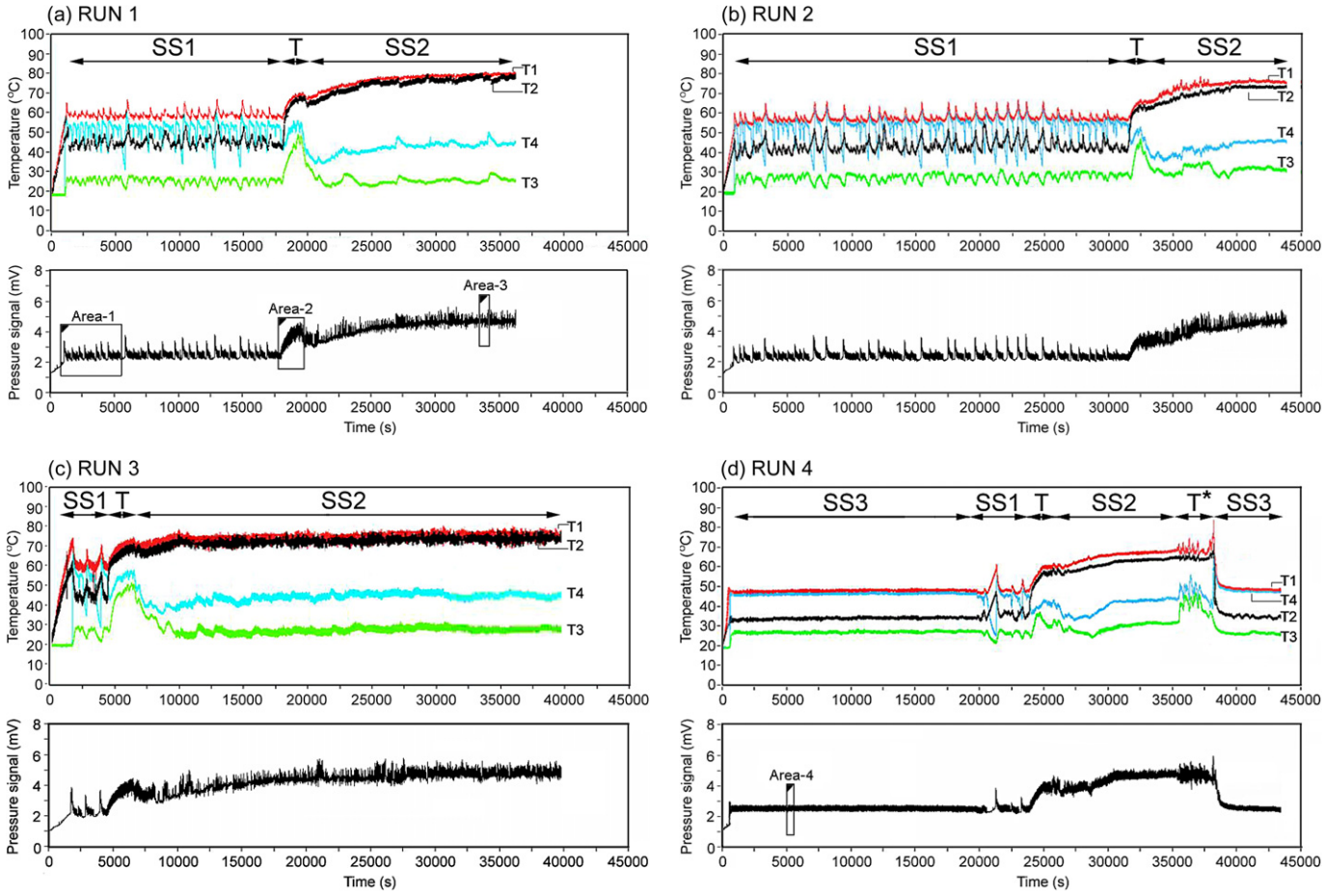

Fig. 2. Variation of temperature and pressure at relevant locations (refer Fig. 1(b)) for four typical runs of CLPHP operation showing existence of distinct steady states.

135 mm, as shown in Fig. 1(b). While the device was mounted on a tiltable frame, the data reported here is only for vertical, heater down configuration. (Note: A single two-phase loop does not run in horizontal and heater-up orientation.) The thermal performance was investigated from the commencement of electrical heating till a quasi-steady state was achieved. Typically, continuous running operational data for 10–12 hours has been recorded and reported here. This continuous operation has manifested different operational steady states and their transient characteristics as described in the next section.

3. Results and discussions

Fig. 2(a)–(d) shows the main results obtained for temporal variation of static pressure at location P and temperature readings of the four thermocouples T1–T4 for four different experimental runs, each at 20 W power input (after accounting for heat losses, which were estimated to be about 8%) and FR $\approx$ 60% of ethanol. The data logging frequency was 100 Hz with simultaneous sampling of all the signals. Although the experiments were performed many times over, these four experimental runs have been chosen as representatives of the main results reported in this study because major observed phenomena are comprehensively covered within the domain of these four runs. As can be clearly seen in Fig. 2, with continuous device operation, multiple quasi-steady states are occurring during the same experimental run without changing any externally controllable parameter. These states are represented by distinct characteristics features of temperature/pressure oscillations, in conjunction with unique flow patterns. These distinctly observed quasi-steady states have been represented by SS1, SS2, SS3 and SS4. In a particular test, after running for sometime, depending on an internal perturbation or an external trigger, the system goes from one quasi-steady state to the other; these jumps have been represented by the transient zones T and T^*. We now describe each of these distinct operating states.

3.1. Start-up zone

After the loop is evacuated and partially filled, the working fluid naturally distributes itself, in the form of liquid plugs and vapor slugs. A typical spatial distribution is as shown in Fig. 3. While we have no control over this initial phase distribution, predominance of surface tension always ensures generation of distinct liquid plugs and vapor slugs/bubbles. Due to surface tension, the vapor slugs/bubbles do not rise up by buoyant forces; the system, if undisturbed, will remain in such a phase distribution for very long time scales [3,10,15]. As we

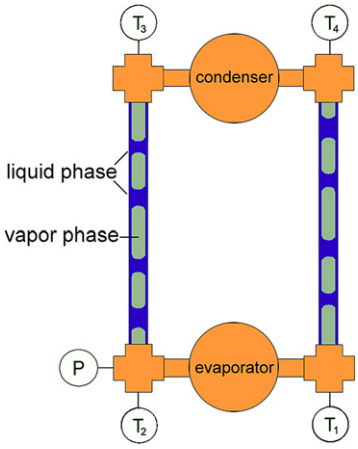

Fig. 3. Initial spatial distribution of the two phases of the working fluid in the loop.

will see later, this initial phase distribution has an important bearing on the overall system dynamics. Initially, with no heat power supplied, the PHP loop is in overall thermal equilibrium and all the four thermocouples show the same initial temperature (i.e. ambient $= 21 \pm 1\,^{\circ}\mathrm{C}$). Having no driving potential (temperature, pressure or density gradient) the two-phase mixture remains stationary. This state is designated as time $t = 0$ s in Fig. 2(a)–(d).

The time span, from $t = 0$ s to the instant when fluid oscillations start and first pressure/temperature fluctuations are observed, is termed as the 'start-up' phase of the PHP. Immediately after $t = 0$ s, DC power is turned on to deliver the desired power (20 W) to the evaporator. In general, two-types of start-ups have been observed (i) gradual start-up, (ii) sudden start-up.

During gradual start-up (as in Runs 1–3), after the power is switched on, it takes considerable time (about 1000 s) for the fluid to start oscillating. The temperature of the evaporator (T1 and T2) keeps rising steadily until a sufficient gradient is setup between the evaporator and condenser temperatures to initiate movement (the condenser block is always supplied with cold fluid at 20 °C). The buoyancy of the hot lighter fluid mixture and bubble nucleation/collapse in the evaporator/condenser zones, respectively, both contribute towards the start-up. This immediately leads to mixing of hot and cold fluid portions causing condenser temperature to increase sharply (depicted as shoot-ups in T3 and T4) with simultaneous decrease in the evaporator temperature, as colder fluid comes down.

During sudden start-up, as seen in experimental Run 4, the above sequence of events take place in a relatively much shorter time period, i.e. the fluid starts oscillating immediately after the heat is turned on.

The occurrence of gradual or sudden start-up depends, most likely, on the initial spatial two-phase distribution of the working fluid in the capillary tube. The presence of liquid–vapor menisci, local void fraction and phase distribution in the evaporator tube at $t = 0$ s seems to be important parameters. More research is required to understand the preference for the system start-up.

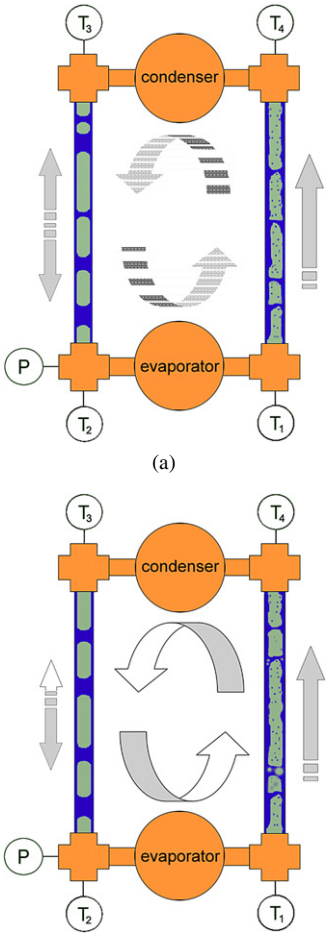

Fig. 4. (a) Flow pattern in steady state 1-unidirectional circulation with quasi-periodic stop-overs. (b) Flow pattern in steady state 3-unidirectional circulation with no stop-over.

3.2. Steady state 1 (SS1)

This steady state is characterized by alternating periods of fluid 'movement' and 'stop-over'. As noted above, the gradual start-up phase commences after a sufficient temperature gradient (ΔT_{E-C}) is established. Commencement of oscillations facilitate mixing of fluid portions in the condenser and the evaporator sections which momentarily again lowers the driving temperature gradient (ΔT_{E-C}) causing the fluid to stop oscillations. As heat is continuously being supplied to the evaporator, this 'stoppage' again causes an increase in evaporator temperature. Thus, the movement/stop-over cycle repeats itself in a quasi-periodic fashion. Phenomenologically, this alternating 'movement' and 'stop-over' mechanism may be compared with classical 'geysering' type static instability in two-phase systems [32].

Fig. 4(a) gives an instantaneous pictorial representation of the flow pattern associated with one operational period or pulsation band of SS1. The overall flow can be described as unidirectional with intermittent stop-overs. The flow tends to take a uniform direction along the right or the left arms. Since the overall average void fraction integrated over the loop is fixed,

i.e. FR $\approx 60\%$, increase in void fraction in the upheader due to heat gain in the evaporator forces the downcomer to have lesser void fraction. Thus, in the upheader, the flow is predominantly churn-annular with frequent liquid bridging while the downcomer has capillary slug flow.

Looking at all the experimental runs (Fig. 2(a)–(d)), another interesting observation is the fact that SS1 does not last for the same time periods in all these experiments. Sometimes it leads to SS2 earlier than in other cases. For example, this transition took place after about 18 000 s in Run 1 while in Run 3 it occurred much earlier, in about 4200 s. In Run 4 we do not observe SS1 at all. At this stage we do not have a complete explanation of these trends. Due to the non-linear nature of the governing thermo-hydrodynamics, a small change in initial conditions and/or interactions of internal perturbations with the flow may cause these transitions. Another corollary is the influence of the start-up behavior of the loop, which in turn, depends on the initial conditions of phase distribution. A close observation reveals that the occurrence of start-up in Run 2 ($\sim$800 s) was the earliest followed by Run 1 ($\sim$1100 s) and then Run 3 ($\sim$1600 s), respectively (Run 4 had the shortest/sudden start-up, which was followed by SS3; this will be discussed in the next section). Since the slope of the transient heating curve leading to a start-up is the same for all the three runs, an early start-up of fluid oscillations essentially means an overall lower operating evaporator temperature. Delayed startup gives higher operating temperature/pressure and a tendency towards an early transition to SS2. (The role of the variation of thermophysical properties of the fluid, for example, effective mixture viscosity, density ratio, vapor mass fraction as a function of vapor void fraction, etc., with temperature is an important consideration in the PHP because the frictional, acceleration and gravitational heads are strongly dependent on it. The linear perturbation analysis of the coupled species transport equation is under development and is therefore not presented here.) Although these observations were recorded for many runs, including those not reported here, further experimental evidence is needed to establish the hypothesis. Typically, the average temperature difference between evaporator and condenser in SS1 was of the order of $\Delta T_{E-C,\mathrm{SS1}} \approx 12\,^{\circ}\mathrm{C}$ which corresponds to an average thermal resistance of $R_{th,\mathrm{SS1}} \approx 0.6\,^{\circ}\mathrm{C/W}$.

3.3. Steady state 3 (SS3)

This steady state is the best operational state of the loop in terms of effective thermal resistance. We take up the description of this state before SS2, as it is, in principle, very similar to SS1 except for the fact that there are no oscillation 'stop-overs'. A typical temperature and pressure response is shown in Run 4 of Fig. 2(d). The ensuing flow pattern in this state of operation, as depicted in Fig. 4(b), is characterized by unidirectional flow circulation with no stop-overs (as were observed during SS1 operation in Runs 1–3). In other words, if the 'pulsating' band of SS1 gets extended unhindered (without any stoppage of fluid oscillations in between) for a long time, it manifests into SS3 operation. During SS3, because of the continuous upward fluid flow in the upheader (right arm as depicted in Fig. 4(b)), both T1 and T4 show nearly the same temperature. Due to small fluid oscillations in the downheader (left arm), some amount of fluid inside the evaporator section flows back or goes up with low-amplitude upward movement making T2 a little warmer than T3. Similar explanation can be given for SS1 (Runs 1–3), where during the pulsation band or operational period, T1 and T4 are nearly similar while T2 and T3 are not. Both, average evaporator temperature ($T_E \approx 40\,^{\circ}\mathrm{C}$) and condenser temperature ($T_C \approx 36\,^{\circ}\mathrm{C}$), are maintained constant throughout SS3; thus $\Delta T_{E-C,\mathrm{SS3}} \approx 4\,^{\circ}\mathrm{C}$ and $R_{th,\mathrm{SS3}} = 0.2\ \mathrm{K/W}$.

In Fig. 2(d) Run 4 data, it can also be seen that SS3 operation is preceded by a very short or nearly sudden startup phase; in fact, the shortest of all the reported experimental runs. Thus, the earlier observation that shorter/immediate start-up of the loop leads to longer stability of a particular steady state and a better thermal performance is further bolstered by observations of Run 4. In many other runs too, which are not reported here, these trends were seen; although we do not have any further irrefutable argument or conclusive theoretical support at this stage to explain this behavior.

3.4. Transition state (T)

During steady state operation (SS1 or SS3), a temperature differential exists between the evaporator and condenser. Due to the colder condenser zone, there is a tendency of liquid-phase accumulation there, leading to enhanced spatial segregation or mal-distribution of the two phases. This accumulation is a result of agglomeration of bubbles as they collapse in the condenser section, leading to larger sized liquid plugs being formed. Whenever such a phenomenon of agglomeration occurs, it momentarily disturbs the void fraction distribution in the remaining portion of the loop. The condenser section gets flooded by a large liquid plug while the evaporator section is starved of liquid inventory. This may, under certain circumstances trigger a transition from one operational steady state to another (SS1 to SS2 or, SS3 to SS1). This event is identified by a sudden change in the flow pattern; it changes from unidirectional flow-circulations to bidirectional flow-reversals.

Fig. 5 shows a pictorial representation of the characteristic flow pattern associated with the transition phase, marked as '*T*' in Fig. 2. Referring to the left side of Fig. 5 which shows an instantaneous depiction, we observe a fluctuating downward slug flow in the downheader (right arm) and churn-annular flow in the upheader (left arm). This situation prevails for some time and then reverses, as shown in right side figure. This direction-reversal or switching occurs in a quasi-periodic fashion. During each flow reversal, condenser being colder has a tendency to hold back more and more liquid phase, i.e. the size of the hanging liquid plug continues to grow (the surface tension is able to hold the weight of the plug at the respective menisci), leaving the evaporator section relatively dryer/hotter. This segregation of the two phases of the working fluid, which disturbs the uniform void distribution, increases the effective thermal resistance of the device and therefore the temperature non-uniformity, depicted as steady increase in the evaporator tem-

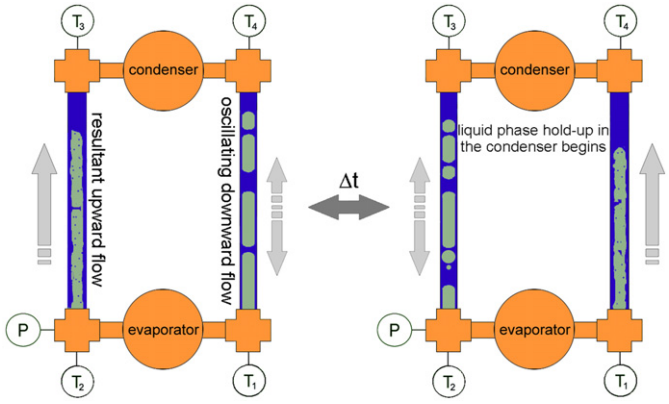

Fig. 5. Flow pattern during the transition phase (T) is characterized by quasi-periodic alternate flow reversals in the upheader and downheader sections.

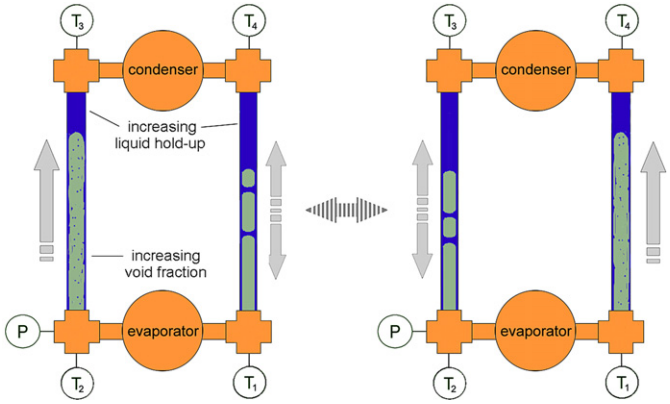

Fig. 6. Flow pattern during steady state-2 shows intermittent flow reversals with a tendency of liquid hold-up in the colder condenser section.

perature and pressure. Increased temperature non-uniformity further catalyzes the process of segregation of the two phases, initiating the commencement of partial/complete dry-out (SS4), or a high thermal resistance operation, marked as 'SS2' in Fig. 2.

3.5. Steady state 2 (SS2)

During the transition phase (T), the liquid hold-up of the condenser section slowly increases. This process degrades heat transfer as colder fluid from the condenser is not able to reach the hot end; the evaporator temperature slowly rises. The quasi-periodic bidirectional flow reversals in the transition phase slowly become erratic and random as the void fraction of the evaporator section continues to increase, and a new steady state, denoted by SS2 is eventually achieved. This steady state is characterized by a near complete phase segregation; very little liquid remains in the evaporator section while a large liquid slug gets held up in the condenser and adjoining adiabatic sections of the loop. Whatever small liquid remains in the evaporator, continues to boil randomly but the disturbance created by the boiling is not sufficient to break the menisci of the hanging liquid plug in the upper colder portion of the loop, as shown in Fig. 6. During SS2, the evaporator and condenser section temperatures are clearly distinguishable as observed in Fig. 2. For 20 W input heat power, temperature non-uniformity during SS2 was observed to be extremely high and is given by $\Delta T_{E-C,\mathrm{SS2}} \approx 40\,^{\circ}\mathrm{C}$, i.e. $R_{th,\mathrm{SS2}} = 2$ K/W. This steady state eventually leads to a complete dry-out of the system, represented by SS4.

3.6. Steady state 4 (dry-out or complete stop-over state)

Because of continuous segregation taking place during SS2, a stage comes when all the liquid-mass is held up in the condenser zone with a long and nearly stagnant vapor plug in the evaporator. This complete segregation of the two phases of the working fluid is termed as the dry-out of the evaporator, pictorially depicted in Fig. 7. Mathematically, this is a trivial solution of the coupled conservation equations guiding the loop operation. As there is no fluid mixing taking place, a steady increase in the evaporator temperature and pressure is observed. The liquid-mass held up in mechanical quasi-equilibrium at the condenser zone is simultaneously acted upon by gravitational body force supported by the vapor pressure in the vapor plug at the two respective menisci. As this is a situation of dynamic equilibrium, it may be disturbed by an external stimuli or an internally generated interface instability which breaks the menisci tension. If sufficient disturbance is present, redistribution of the two phases of the working fluid can take place, causing system to go back to operate under a different steady state (i.e. SS1, SS2 or SS3) depending upon the extent of spatial phase distribution homogeneity achieved through the mixing.

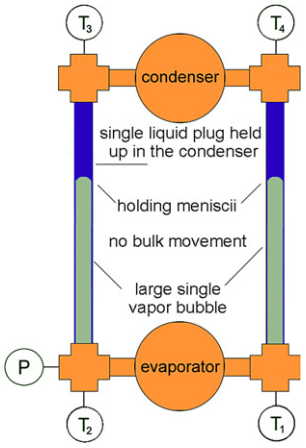

Fig. 7. Complete segregation of the two phases of the working fluid, leading to evaporator dryout (steady state 4).

In Fig. 2(d), we observe that continuous running in SS2 slowly leading the system to SS4. As the liquid hold-up of the condenser increases during SS2, the thermal resistance of the system increases. Eventually at around 35 500 s, partial dryouts of the evaporator are clearly seen with evaporator temperature and pressure grossly fluctuating. These fluctuations are caused because the interface instability at the menisci forces a small amount of liquid-mass to fall down by gravity to the evaporator. This instantaneously flashes into vapor causing the violent fluctuations of pressure and temperature. This intermittent flashing of the liquid accompanied with the sudden drop and rise in the evaporator temperature and vapor pressure is marked by T^* in

Fig. 2(d). While these events continue for some time, at about 38 000 s, there is a sudden drop in the evaporator pressure, shoot-up in the condenser temperature (T3 and T4) and simultaneous drop in the evaporator temperature (T1 and T2); the system goes back to steady state operation SS3.

4. Temporal scaling and frequency analysis

As is seen from the operational characteristics, thermo-hydrodynamics of a CLPHP loop involves various transient processes which are intrinsically non-linear and coupled. These processes, on a time averaged basis, give the overall thermal performance in terms of thermal resistance of the device. The fact that the tube is joined end-to-end necessitates that the time averaged void fraction integrated along the loop must correspond to the initial void fraction at the time of filling the device [3,33]. Also, the net flow velocity obtained at any instant is not known a priori and comes out as a solution of the coupled transport equation of the loop. For the purpose of scaling analysis, we need an effective time scale of the device under different operating conditions so that an applicable velocity scale may be estimated from the known length scale corresponding to the geometry of the device.

To obtain a suitable time scale, we consider the fact that the phase change phenomenon on the evaporator tube may be considered as a 'chemical reaction' in which the liquid particles are continuously disappearing into vapor molecules with a certain 'rate of reaction' governed by the input heat flux, latent heat of vaporization and the geometry of the evaporator. Thus, drawing an analogy with the Damköhler number of group I in chemical kinetics [34], the mass rate of vapor generation per unit volume (rate of reaction under thermodynamic equilibrium conditions) is given by:

$$\Gamma_{\text{vap}|\text{eq}} = \left(\frac{\dot{q}''_w \cdot \xi_h}{A \cdot h_{fg}}\right) = \left(\frac{4 \cdot \dot{q}''_w}{D_{\text{hyd}} \cdot h_{fg}}\right) \tag{1}$$

This 'rate of reaction' may be divided by the local mass concentration, i.e. two-phase mixture density, to give the frequency of phase change as,

$$\Omega_{\text{eq}} = \left(\frac{\Gamma_{\text{vap}|\text{eq}}}{\rho_{2\text{-}\phi}}\right) \tag{2}$$

Similar analysis done by Saha et al. [35] leads to equilibrium phase change number,

$$N_{pc}|_{\text{eq}} = \Omega_{\text{eq}} \cdot \left(\frac{L}{v_{\text{liq,in}}}\right) \tag{3}$$

In their analysis, Saha et al. [35] have explored the stability of vaporizing flows with respect to density-wave oscillations in circular channels that are open at both ends. While the general phenomenological conclusion of their perturbation analysis fits well to the present case of pulsating heat pipes, the inlet velocity of flow, which was explicitly known in their case (the flow entered as single phase liquid in a heated pipe from one end with known velocity and exited from the other end as a two-phase mixture), is unavailable for CLPHP analysis. Also, in contrast, the inlet to the evaporator is typically always under two-phase flow conditions in a CLPHP and is different and changing for each evaporator U-turn (in a multi-turn device). Therefore, in general, any non-dimensional number having the explicit inclusion of the velocity is not suitable for CLPHP analysis as this quantity is not known a priori. Furthermore, the level of fluid inlet subcooling to the evaporator section, which is known to affect the stability criteria of two-phase flows, is also unknown (and variable!) in the present case. Nevertheless, the equilibrium frequency of phase change provides a convenient time scale. To illustrate this, we plug-in the actual thermophysical data for ethanol at 80 °C operating temperature, in Eq. (1) ($\dot{q}''_w = 20/(\pi \cdot 2\text{e}^{-3} \cdot 80\text{e}^{-3}) \approx 40\,000$ W/m^2, $D_{\text{hyd}} = 2\text{e}^{-3}$ m and $h_{fg} = 960$ kJ/kg) to get,

$$\Gamma_{\text{vap}|\text{eq}} = \left(\frac{4 \cdot \dot{q}''_w}{D_{\text{hyd}} \cdot h_{fg}}\right) \approx \left(\frac{4 \cdot 40\,000}{2\text{e}^{-3} \cdot 960\text{e}^{3}}\right) \approx 83 \text{ kg/s m}^3 \tag{4}$$

For an initial filling ratio of sixty percent, i.e. void fraction $\alpha = 0.4$, considering that $\rho_{\text{liq}} = 780$ kg/m^3 and $\rho_{\text{vap}} = 1.3$ kg/m^3, the vapor mass fraction x scales as 1.0e–4, as given by Eq. (5),

$$\left(\frac{x}{1-x}\right) = \left(\frac{\alpha}{1-\alpha}\right)\left(\frac{\rho_{\text{vap}}}{\rho_{\text{liq}}}\right)\bar{K} \tag{5}$$

where, $\bar{K} = (v_{\text{vap}}/v_{\text{liq}})$ is the slip factor of the two-phases. Commensurate with homogeneous ($\bar{K} = 1$) or a separated flow model ($\bar{K} \approx 1.1$–1.5 for capillary slug flows [32,36]) for two-phase flow in the evaporator, an increase in vapor mass fraction x in the evaporator will substantially increase the local void fraction. Thus, effective two-phase flow density given by:

$$\rho_{2\text{-}\phi} = \alpha\rho_{\text{vap}} + (1-\alpha)\rho_{\text{liq}} \tag{6}$$

is expected to be of the order of $\rho_{2\text{-}\phi} \approx 500$ to 25 kg/m^3. Therefore, the frequency of phase change is expected to be of the order of:

$$\Omega_{\text{eq}} = \left(\frac{\Gamma_{\text{vap}|\text{eq}}}{\rho_{2\text{-}\phi}}\right) \approx 0.15 \text{ to } 3.5 \text{ Hz} \tag{7}$$

Thus, a simple scaling analysis presented above, albeit with many inherent simplifications and assumptions [35], including thermodynamic equilibrium between the two-phases, does suggests that the PHP loop may manifest multiple phase change frequencies depending on the heat flux, geometry, local void fraction which is experienced by the evaporator (the void fraction may increase either by increasing the heat flux or by a change in phase distribution in the loop, caused, for example, by liquid hold-up in the condenser) and the operating temperature of the loop which affects the thermophysical properties of the working fluid.

To ascertain the validity of the above scaling estimates, we analyzed the pressure data presented in Runs 1–4 to get their spectral contents. The sections represented by Area-1, Area-2 and Area-3 and Area-4 in Fig. 2(a)–(d) are separately represented by Figs. 8 and 9 along with the corresponding power spectrum of pressure signal. The following salient features may be noted from this analysis:

(i) Major spectral content of the CLPHP system is indeed between the range 0.1–3 Hz, as suggested by the scaling

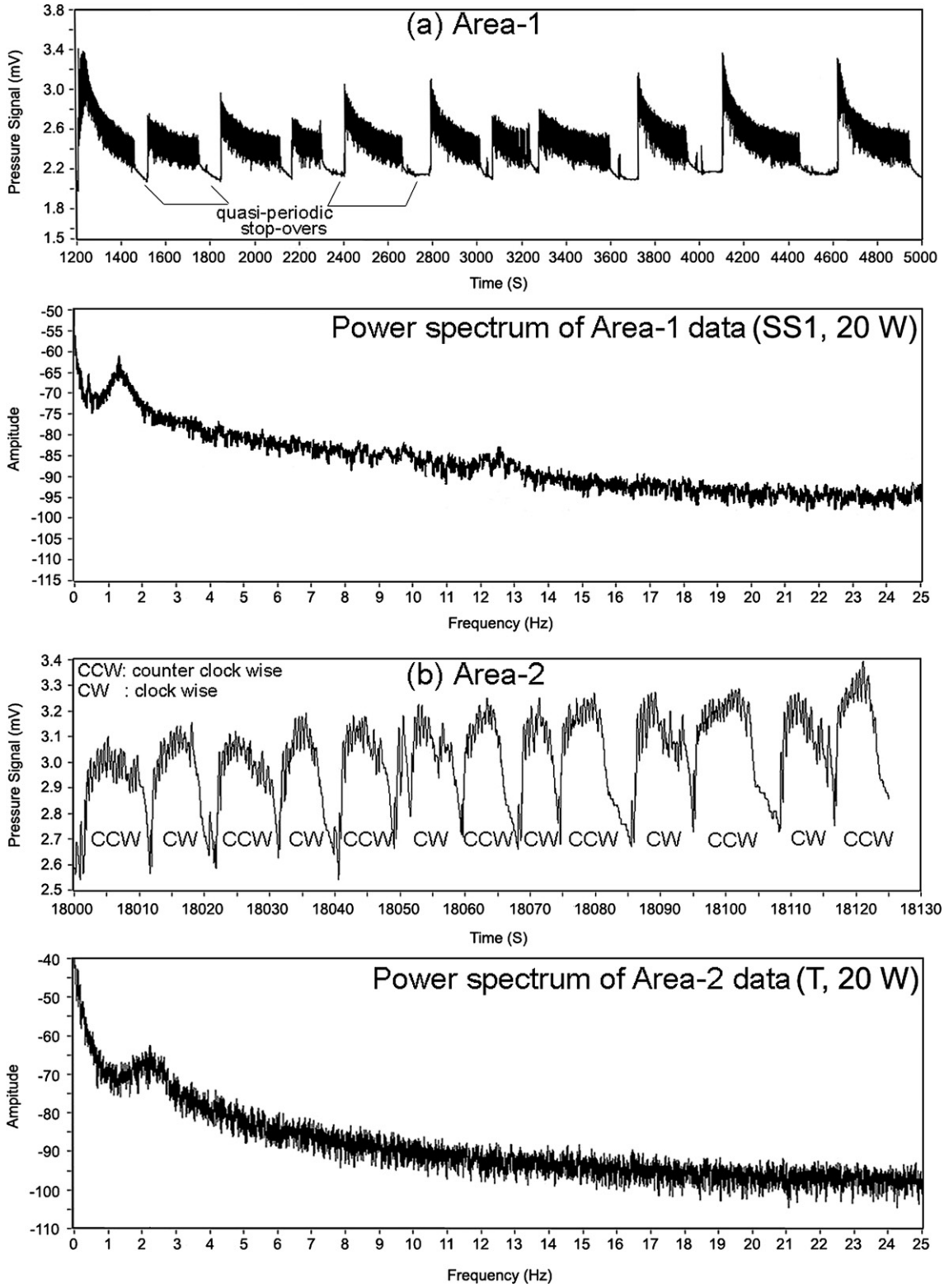

Fig. 8. Magnified view of pressure variation in (a) Run 1–Area-1 data of SS1 and its power spectrum, and (b) Area-2 data of transient condition T and its power spectrum (refer Fig. 2).

estimate above. (At this stage, it should also however be noted that the scaling analysis as presented here only provides an 'order of magnitude' estimates of the time scales involved in the system dynamics.) Since the length scale of the device is of the order of 200 mm, this suggests that the velocity scales are of the order of 20 to 600 mm/s. We have conducted initial studies on measurement of slug velocity by slow motion videography and these estimates are inline with the measurements. Further detailed work in this direction is indeed needed to confirm and establish

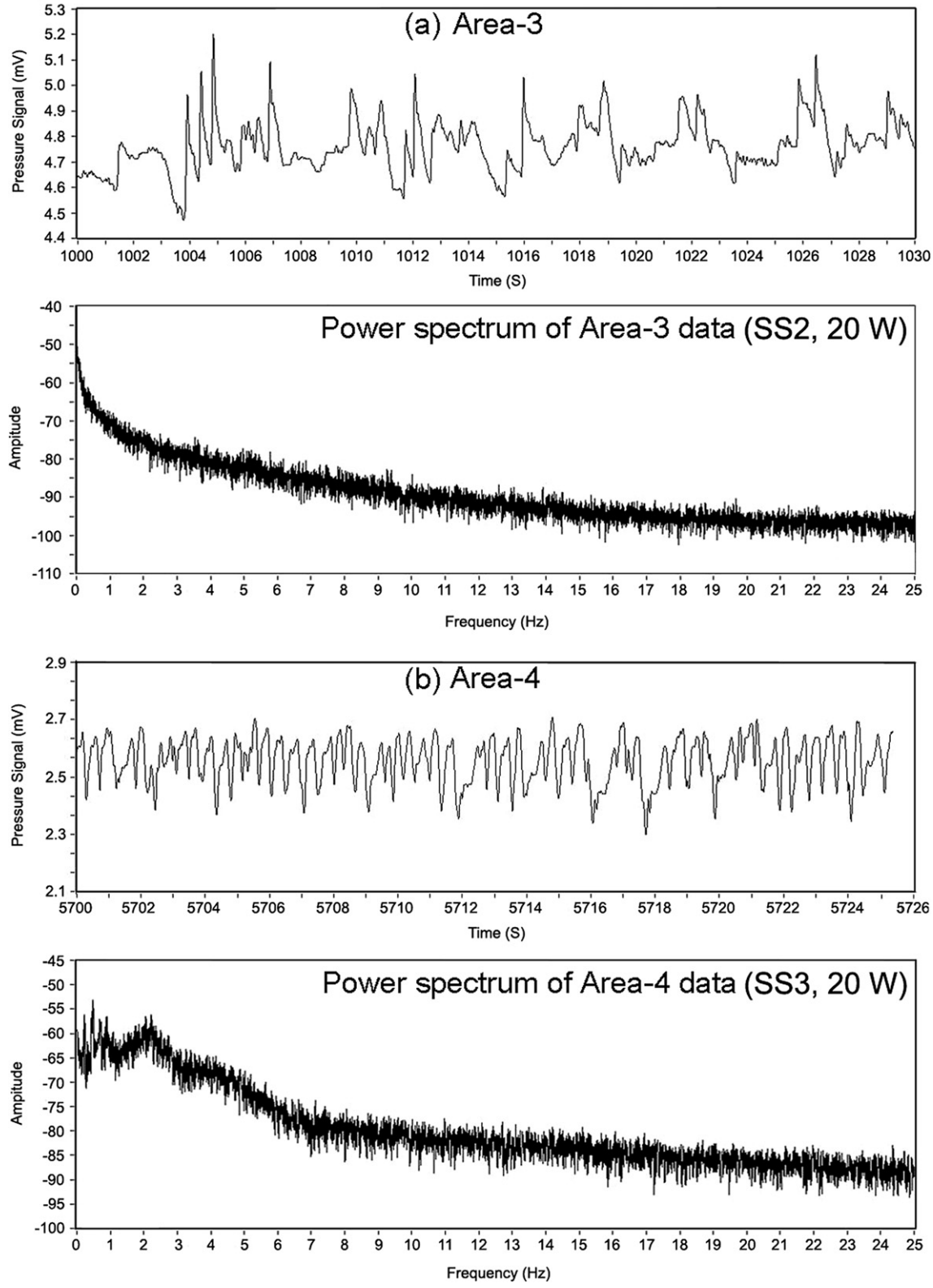

Fig. 9. Magnified view of pressure variation in (a) Run 1–Area-3 data of SS2 and its power spectrum, and (b) Run 4–Area-4 data of SS3 and its power spectrum (refer Fig. 2).

these velocity estimates. Nevertheless, results reported by Xu et al. [37] and Lips and Bonjour [38] do confirm the order of magnitude of average two-phase flow velocity in the single PHP loop. Xu et al. [37] also report qualitatively that while bubble displacements and velocities do display periodic oscillations, these are superimposed by multiple frequencies which depend on operating parameters. Lips and Bonjour [38] have considered a simple one-

dimensional slug flow model of a PHP and their analysis highlights the presence of operating parameters dependent eigen frequencies in the system. In another study, Xu and Zhang [39] report experimental and numerical study on start-up and steady thermal oscillations on a 2.0 mm PHP with FC-72 as the working fluid. Their results not only indicate the presence of two distinct types of start-ups, the spectral contents of the oscillations are also reported to be between 0.09–1 Hz, depending on the applied boundary conditions. These studies strongly compliment the present findings.

(ii) Steady state 2, which corresponds to the worst thermal performance, has no dominant frequency of phase change. The flow oscillations are aperiodic and random, as has been explained in Section 3.5.

(iii) In Steady state 1 (Area-1, Fig. 8(a)), quasi-periodic flow stop-overs are clearly visible. The periods for such stop-overs are typically in the range of 200 to 400 s which corresponds to very low frequency. The peak frequencies of 0.4 and 1.6 Hz correspond to the flow oscillations during the stop-overs.

(iv) The best operating steady state (SS3) has multiple dominant frequencies between 0.1–2.2 Hz. Pressure variation data (Area-4) suggests smooth operation with no stop-overs of the flow.

(v) In the transition phase (T) bidirectional flow reversals are seen, represented by CCW and CW in Fig. 8(b). While these flow reversals take place at very low frequency, a frequency of 2.5 Hz corresponds to the flow oscillations observed in the upheader/downheader during a particular CC or CCW operation.

5. Summary and conclusions

A single two-phase capillary loop, representing the building block of a multi-turn pulsating heat pipe was constructed and tested under controlled conditions for continuous long durations. Online temperature measurements at important locations and absolute pressure measurement at the inlet to the evaporator were done along with simultaneous flow visualization. For the results reported in this work, the filling ratio, working fluid, device orientation and the heating input to the loop was kept constant. The following main conclusions can be drawn from the study:

(1) For a fixed set of operating/boundary conditions, the single turn device is observed to operate under multiple steady states. Four distinct steady states, named SS1–SS4 respectively, have been observed. Each steady state is characterized by a specific, definite flow pattern and associated effective thermal resistance. While the loop continues to operate under one steady state, under certain conditions, triggered by external or internal flow perturbations, transition from one steady state to the other is observed. This event (transition phase T) is identified by a change in the flow pattern and therefore the thermal resistance of the device.

(2) Two types of loop start-ups were observed, (a) a 'sudden start-up' in which the two-phase flow oscillations start relatively early after the application of heat, and (b) a 'gradual start-up' wherein the first flow oscillations commence with relatively more delay time after the application of heat. In general, a quick start-up corresponds to a lower loop operating temperature and more stable operation at low thermal resistance. These start-ups are dependent on the initial phase distribution in the loop.

(3) Steady state operation with higher thermal resistance is usually an outcome of an uneven phase distribution inside the loop. Liquid hold-up in the colder condenser zone has been observed to be the primary cause for the initiation of an uneven phase distribution in the loop during operation. Thus, sustenance of homogeneous two-phase distribution in the loop leads to an overall improved performance.

(4) A continuous unidirectional flow circulation is associated with the least thermal resistance operation (i.e. SS3) which enables continuous transfer of heat from the evaporator section to the condenser. Therefore, temperature non-uniformity (or, effective thermal resistance) of the device is very small. State SS1 is also characterized to possess unidirectional flow-circulations but with quasi-periodic stop-overs in between. These stop-overs interrupt the continuous heat transfer, which explains a little higher effective thermal resistance of the PHP operating under SS1 as compared to SS3.

(5) Complete dryout of the device is one of the 'steady states' of the loop. In such a situation there is a single liquid plug which hangs in the cooler condenser zone while the evaporator section is covered up by one vapor bubble. There is no bulk movement; the two separating menisci only occasionally oscillate around a mean position. The evaporator temperature exceeds the safe limits and the heating of the device has to be stopped if this state continues for a long time. Meanwhile, if the holding menisci are sufficiently perturbed, the hanging liquid-mass may fall down to the evaporator zone and phase redistribution may occur, leading to transition back to an operating steady state.

(6) Spectral contents of the pressure transducer signal reveals oscillating frequencies ranging from 0.1 Hz to 3 Hz. Each steady state consists of a representative unique power spectrum. The visualization sequences also indicate to similar order of magnitude of frequency contents. While, an 'order of magnitude' estimation of the spectral contents can be conveniently done by scaling provided by the equilibrium frequency of phase change, more analyses is needed to decipher the full signature of the ensuing oscillations.

The results presented in this work have profound implications on the understanding of the thermo-physics of multi-turn pulsating heat pipes. Whether a multi-turn device will also exhibit multiple steady states remains to be seen. The perturbing effect of number of turns coupled with bubble pumping/collapsing force is not fully understood at this stage. Fundamental modeling and subsequent stability maps need to be

addressed in the light of the singular behavior manifested by the capillary two-phase loop.

Acknowledgements

The work is partially supported by financial grants from Indian Space Research Organization (ISRO/ME/20050083) and Board of Research for Nuclear Sciences, India (BRNS/DAE/20050292). The second author received graduate fellowship under DGF Scheme, Department of Atomic Energy, Government of India. Technical help from Mr. C.S. Goswami is appreciated.

References

[1] H. Akachi, US patent, Number 5490558, 1996.
[2] M. Groll, S. Khandekar, Heat transfer and fluid flow in microchannels: Micro heat pipes, Heat Exchanger Design Handbook (HEDU-Update) 9 (1–2) (2002).
[3] S. Khandekar, Thermo-hydrodynamics of closed loop pulsating heat pipes, Doctoral dissertation, Universitaet Stuttgart, Germany, 2004; available online at http://elib.uni-stuttgart.de/opus/volltexte/2004/1939/.
[4] L.L. Vasiliev, Heat pipes in modern heat exchangers, Applied Thermal Engineering 25 (2005) 1–19.
[5] B.Y. Tong, T.N. Wong, K. Ooi, Closed-loop pulsating heat pipe, Applied Thermal Engineering 21 (18) (2001) 1845–1862.
[6] L. Lin, Experimental investigation of oscillation heat pipes, J. Thermophys. Heat Transfer 15 (2001) 395–400.
[7] S. Khandekar, N. Dollinger, M. Groll, Understanding operational regimes of pulsating heat pipes: An experimental study, Applied Thermal Engineering 23 (6) (2003) 707–719.
[8] P. Charoensawan, S. Khandekar, M. Groll, P. Terdtoon, Closed loop pulsating heat pipes. Part A: Parametric experimental investigations, Applied Thermal Engineering 23 (16) (2003) 2009–2020.
[9] D. Reay, P. Kew, Heat Pipes, fifth ed., Butterworth-Heinemann, 2006, ISBN 10:0750667540.
[10] Q. Cai, C.L. Chen, J.F. Asfia, Operating characteristic investigations in pulsating heat pipe, ASME Journal of Heat Transfer 128 (12) (2006) 1329–1334.
[11] W. Qu, Y. Zhou, Y. Li, T. Ma, Experimental study on mini pulsating heat pipes with square and regular triangle capillaries, in: Proc. 14th International Heat Pipe Conference (IHPC), Florianopolis, Brazil, 2007.
[12] S. Khandekar, M. Groll, An insight into thermo-hydraulic coupling in pulsating heat pipes, International Journal of Thermal Sciences 43 (1) (2004) 13–20.
[13] S. Maezawa, F. Sato, K. Gi, Chaotic dynamics of looped oscillating heat pipes (theoretical analysis on single loop), in: Proc. 6th Int. Heat Pipe Symp., Chiang Mai, Thailand, 2000, pp. 273–280.
[14] S. Khandekar, M. Groll, P. Charoensawan, P. Terdtoon, Pulsating heat pipes: Thermo-fluidic characteristics and comparative study with single phase thermosyphon, in: Proc. 12th Int. Heat Transfer Conf., ISBN-2-84299-307-1, vol. 4, Grenoble, France, 2002, pp. 459–464.
[15] H. Akachi, F. Polášek, P. Štulc, Pulsating heat pipes, in: Proc. 5th Int. Heat Pipe Symp., Melbourne, Australia, 1996, pp. 208–217.
[16] S. Khandekar, M. Groll, Insights into the performance modes of closed loop pulsating heat pipes and some design hints, in: Proc. 18th National & 7th ISHMT-ASME Heat and Mass Transfer Conference, Guwahati, India, 2006.
[17] M. Hosoda, S. Nishio, R. Shirakashi, Study of meandering closed-loop heat-transport device (vapor-plug propagation phenomena), JSME Int. Journal, Series B 42 (4) (1999) 737–743.
[18] M.B. Shafii, A. Faghri, Y. Zhang, Thermal modeling of unlooped and looped pulsating heat pipes, ASME J. Heat Trans. 123 (2001) 1159–1172.
[19] S. Khandekar, M. Schneider, P. Schaefer, R. Kulenovic, M. Groll, Thermofluiddynamic study of flat plate closed loop pulsating heat pipes, Microscale Thermophysical Engineering 6/4 (2002) 303–318.
[20] Y. Zhang, A. Faghri, Heat transfer in a pulsating heat pipe with open end, Int. J. Heat Mass Transfer 45 (2002) 755–764.
[21] H. Yang, S. Khandekar, M. Groll, Operational limit of closed loop pulsating heat pipes, Applied Thermal Engineering 28 (2008) 49–59.
[22] P. Sakulchangsatjatai, N. Kammuanglue, P. Terdtoon, D.J. Mook, Effect of geometrical sizes on maximum heat flux of a vertical closed loop pulsating heat pipe, in: Proc. 14th International Heat Pipe Conference (IHPC), Florianopolis, Brazil, 2007.
[23] A. Bensalem, C. Romestant, A. Alexandre, Y. Bertin, Experimental investigation of pulsating heat pipes, in: Proc. 14th International Heat Pipe Conference (IHPC), Florianopolis, Brazil, 2007.
[24] R. Grief, Natural circulation loops, ASME Trans. J. Heat Transfer 110 (1988) 1243–1258.
[25] Y.Y. Jiang, M. Shoji, Spatial and temporal stabilities of flow in a natural circulation loop: Influences of thermal boundary condition, Journal of Heat Transfer 125 (2003) 612–623.
[26] R. Waschler, S. Pushpavanam, A. Kienle, Multiple steady states in two-phase reactors under boiling conditions, Chemical Engineering Science 58 (11) (2003) 2203–2214.
[27] A. Baars, A. Delgado, Multiple modes of a natural circulation evaporator, Int. Journal of Heat Mass Transfer 49 (2006) 2304–2314.
[28] L.L. Tong, T.S. Li, X.Y. Li, Non-dimensional analysis of static bifurcation in a natural circulation loop, Nuclear Science and Technology 17 (1) (2006) 61–64.
[29] G.P. Mehta, A.B. Eisenhower, Computational modeling and analysis of multiple steady states in vapor compression systems, Journal of Computational and Non-Linear Dynamics 2 (2007) 132–140.
[30] M. Misale, P. Garibaldi, J.C. Passos, G. Ghisi de Bitencourt, Experiments in a single-phase natural circulation mini-loop, Experimental Thermal and Fluid Sciences 31 (2007) 1111–1120.
[31] J. Boure, A. Bergles, L. Tong, Review of two-phase flow instability, Nuclear Eng. Design 25 (1973) 165–192 (also ASME paper No 71-HAT-42).
[32] P. van Carey, Liquid Vapor Phase Change Phenomena, second ed., Taylor and Francis, ISBN 1591690358, 2007.
[33] S. Khandekar, S. Manyam, M. Groll, M. Pandey, Two-phase modeling in closed loop pulsating heat pipes, in: Proc. 13th Int. Heat Pipe Conf., Shanghai, China, 2004.
[34] H. Fogler Scott, Elements of Chemical Reaction Engineering, fourth ed., Prentice-Hall, 2005, ISBN 10:0130473944.
[35] P. Saha, M. Ishii, N. Zuber, An experimental investigation of the thermally induced flow oscillations in two-phase systems, ASME J. Heat Transfer 98 (1976) 616–622.
[36] G. Wallis, One-Dimensional Two Phase Flow, McGraw-Hill, 1969.
[37] J.L. Xu, Y.X. Li, T.N. Wong, High speed flow visualization of a closed loop pulsating heat pipe, Int. J. Heat Mass Transfer 48 (2005) 3338–3351.
[38] S. Lips, J. Bonjour, Oscillating two-phase flow in a capillary tube: Experiments and modeling, in: Proc. 14th International Heat Pipe Conference (IHPC), Florianopolis, Brazil, 2007.
[39] J.L. Xu, X.M. Zhang, Start-up and steady thermal oscillation of a pulsating heat pipe, Heat and Mass Transfer 41 (8) (2005) 685–694.